

## Metadata of the article that will be visualized in OnlineFirst

1	Article Title	<b>The Use of Sodium to Calibrate the Transport Modeling of Water Pollution in Sandy Formations Around an Uninsulated Sewage Disposal Site</b>		
2	Article Sub- Title			
3	Article Copyright - Year	<b>Springer International Publishing Switzerland 2016 (This will be the copyright line in the final PDF)</b>		
4	Journal Name	Water, Air, & Soil Pollution		
5	Corresponding Author	Family Name	<b>Szabó</b>	
6		Particle		
7		Given Name	<b>György</b>	
8		Suffix		
9		Organization	University of Debrecen	
10		Division	Department of Landscape Protection and Environmental Geography	
11		Address	Egyetem Square 1, Debrecen 4010	
12		e-mail	szabo.gyorgy@science.unideb.hu	
13	Author	Family Name	<b>Bessenyei</b>	
14		Particle		
15		Given Name	<b>Éva</b>	
16		Suffix		
17		Organization	University of Debrecen	
18		Division	Department of Landscape Protection and Environmental Geography	
19		Address	Egyetem Square 1, Debrecen 4010	
20		e-mail		
21	Author	Family Name	<b>Hajnal</b>	
22		Particle		
23		Given Name	<b>Andor</b>	
24		Suffix		
25		Organization	University of Debrecen	
26		Division	Department of Mineralogy and Geology	
27		Address	Egyetem Square 1, Debrecen 4010	
28		e-mail		
29	Author	Family Name	<b>Csige</b>	

30		Particle	
31		Given Name	<b>István</b>
32		Suffix	
33		Organization	Institute for Nuclear Research of the Hungarian Academy of Science, Department of Earth and Environmental Sciences
34		Division	
35		Address	Bem tér 18/c, Debrecen 4026
36		e-mail	
37		Family Name	<b>Szabó</b>
38		Particle	
39		Given Name	<b>Gergely</b>
40		Suffix	
41	Author	Organization	University of Debrecen
42		Division	Department of Physical Geography and Geoinformatics
43		Address	Egyetem Square 1, Debrecen 4010
44		e-mail	
45		Family Name	<b>Tóth</b>
46		Particle	
47		Given Name	<b>Csaba</b>
48		Suffix	
49	Author	Organization	University of Debrecen
50		Division	Department of Physical Geography and Geoinformatics
51		Address	Egyetem Square 1, Debrecen 4010
52		e-mail	
53		Family Name	<b>Posta</b>
54		Particle	
55		Given Name	<b>József</b>
56		Suffix	
57		Organization	University of Debrecen
58	Author	Division	Department of Landscape Protection and Environmental Geography
59		Address	Egyetem Square 1, Debrecen 4010
60		Organization	University of Debrecen
61		Division	Department of Inorganic and Analytical Chemistry
62		Address	Egyetem Square 1, Debrecen 4010
63		e-mail	
64	Author	Family Name	<b>Mester</b>
65		Particle	

66	Given Name	<b>Tamás</b>
67	Suffix	
68	Organization	University of Debrecen
69	Division	Department of Landscape Protection and Environmental Geography
70	Address	Egyetem Square 1, Debrecen 4010
71	e-mail	
72	Received	19 August 2015
73	Schedule	Revised
74		Accepted 21 December 2015
75	Abstract	In the present paper we suggest a novel calibration method of the model for hydrodynamic and contaminant transport using the example of a sewage disposal site set up uninsulated in a sandy environment. With the hydrodynamic model we applied time-dependent model calculations in order to fit the individual hydrodynamic parameters. For the calibration of the transport model, sodium was chosen, which has a negligible retardation factor. We demonstrated that this approach is suitable for creating a model that provides calculated results comparable to the actually measured, experimental ones. The created model proved to be appropriate for use in the estimation of the maximal spatial extension of the contamination, which—in the case of the investigated sewage disposal site—was found to be 0.1 km <sup>2</sup> in the near-surface (1–3 m deep) layers, whereas it was three times higher at a depth of 40–60 m.
76	Keywords separated by ' - '	Contamination transport - Groundwater pollution - Model calibration - Sewage disposal site - Sodium
77	Foot note information	

# The Use of Sodium to Calibrate the Transport Modeling of Water Pollution in Sandy Formations Around an Uninsulated Sewage Disposal Site

György Szabó · Éva Bessenyei · Andor Hajnal · István Csige ·  
Gergely Szabó · Csaba Tóth · József Posta · Tamás Mester

Received: 19 August 2015 / Accepted: 21 December 2015  
© Springer International Publishing Switzerland 2016

**Abstract** In the present paper we suggest a novel calibration method of the model for hydrodynamic and contaminant transport using the example of a sewage disposal site set up uninsulated in a sandy environment. With the hydrodynamic model we applied time-dependent model calculations in order to fit the individual hydrodynamic parameters. For the calibration of the transport model, sodium was chosen, which has a negligible retardation factor. We demonstrated that this approach is suitable for creating a model that provides calculated results comparable to the actually measured, experimental ones. The created model proved to be

appropriate for use in the estimation of the maximal spatial extension of the contamination, which—in the case of the investigated sewage disposal site—was found to be 0.1 km<sup>2</sup> in the near-surface (1–3 m deep) layers, whereas it was three times higher at a depth of 40–60 m.

**Keywords** Contamination transport · Groundwater pollution · Model calibration · Sewage disposal site · Sodium

## 1 Introduction

The anthropogenic contamination of groundwater presents a serious problem in many locations worldwide (Datta et al. 2011; Delkash et al. 2014). Contaminants of agricultural and industrial origin can frequently be found lying behind this problem (Al-Khashman 2008); in addition, the lack of any sewerage installation, poorly insulated or even uninsulated communal septic tanks, sewage disposal sites lacking proper technological protection, and landfills for solid waste materials can also pose a threat and may seriously contaminate the groundwater (Phan et al. 2013, 2014). The rate and severity of contamination can reach such levels that in and around settlements the groundwater may become unsuitable not only for human or animal consumption but also for irrigation (Somlyódi 2002). Of the various groundwater types, shallow groundwater is the most at risk, because it is usually located near the surface and contaminants from the topsoil are first transferred here via water

G. Szabó (✉) · É. Bessenyei · J. Posta · T. Mester  
Department of Landscape Protection and Environmental  
Geography, University of Debrecen, Egyetem Square 1,  
Debrecen 4010, Hungary  
e-mail: szabo.gyorgy@science.unideb.hu

A. Hajnal  
Department of Mineralogy and Geology, University of Debrecen,  
Egyetem Square 1, Debrecen 4010, Hungary

I. Csige  
Institute for Nuclear Research of the Hungarian Academy of  
Science, Department of Earth and Environmental Sciences, Bem  
tér 18/c, Debrecen 4026, Hungary

G. Szabó · C. Tóth  
Department of Physical Geography and Geoinformatics,  
University of Debrecen, Egyetem Square 1, Debrecen 4010,  
Hungary

J. Posta  
Department of Inorganic and Analytical Chemistry, University of  
Debrecen, Egyetem Square 1, Debrecen 4010, Hungary

55 infiltration (Cho et al. 2000; Kerényi 2003; Slack et al.  
56 2005, 2007; Fejes et al. 2012).

57 To control the quality of groundwater and to follow  
58 the transport of possible contaminants, the operation of a  
59 monitoring network is essential. At the same time, the  
60 interpretation of the measurement results requires the  
61 formulation of a conceptual geological model. If a math-  
62 ematical model based on this conceptual model is also  
63 available, it enables significant further qualitative anal-  
64 yses. Over the last few decades, due to the rapid devel-  
65 opment of computer science, the creation of such  
66 models—and their practical application in the solution  
67 of groundwater-protection problems—has become more  
68 and more frequent (Shahid et al. 2000; Sonneveld et al.  
69 2010; Zhang et al. 2013). In order to protect groundwa-  
70 ter, it is vital to ensure both the geological and the  
71 technological protection of the waste disposal sites  
72 (Panno et al. 2002, 2006; Sipos et al. 2012; Chawla  
73 and Singh 2014). This statement is supported by the  
74 research conducted by Regadio et al. (2011) and Zhan  
75 et al. (2013) in sampling locations in Spain and south-  
76 eastern China, respectively, in the areas surrounding  
77 operational waste disposal sites. In India, the high arse-  
78 nic (As) content of the groundwater can cause serious  
79 problems, and to understand these processes,  
80 researchers have relied on three-dimensional hydrody-  
81 namic and transport models that work with finite-  
82 difference methods, which have long been established  
83 in Japan (Nakaya et al. 2011). Chakraborty and Ghosh  
84 (2009) also worked with software that uses a finite-  
85 difference method, to model chloride and sodium trans-  
86 port in the vicinity of a municipal solid waste landfill.

87 The present research was conducted in the area of a  
88 sewage disposal site that had been operational for almost  
89 three decades and then recultivated. Based on the avail-  
90 able measurement results, the main aim of our study was  
91 to establish a calibration procedure that would signifi-  
92 cantly improve the reliability of the contaminant trans-  
93 port model currently in use. A further aim was to use this  
94 newly calibrated model to assess the main characteris-  
95 tics of the spatial and temporal changes in water quality  
96 and the development of the clarifying process following  
97 recultivation. The latter is even more important as there  
98 is surprisingly little information available in the litera-  
99 ture with regard to the actual size of the affected area of  
100 such a contamination source in sandy zones. The rate of  
101 water quality improvement after a recultivating inter-  
102 vention is also rather unclear. Thus, these investigations  
103 may provide a solid basis for the assessment of risks due

to the contamination of artesian waters and also for the 104  
establishment of the need for a possible future 105  
intervention. 106

**2 Materials and Methods** 107

2.1 Description of the Study Area 108

The area we studied is found in eastern Hungary, 8 km 109  
south of Debrecen, in the administrative township of 110  
Mikepércs (Fig. 1). Regarding its geological structure, it 111  
is a S-SW sloping, sand-covered alluvial fan plain of 112  
aeolian origin. The climate of the area is warm temper- 113  
ate and dry temperate; the mean annual temperature is 114  
9.8–10.0 °C, and the average annual rainfall is 550– 115  
580 mm (Dövényi 2010). Between 1982 and 2011, the 116  
hole of an abandoned sandpit was used as a disposal site 117  
for the wastewater produced by the town, the quantity of 118  
which even exceeded a daily 100 m<sup>3</sup>. This sewage 119  
disposal site had been established and used without 120  
any authorization, and had no technological protection. 121  
The sewage disposal site with a total capacity of 122  
20,000 m<sup>3</sup> was formed on a sandy soil structure, and 123  
under such conditions the contaminants could easily 124  
infiltrate into the groundwater. Previous studies from 125  
2004, 2005, and 2010 justified that, as a consequence 126  
of the sewage disposal, the groundwater became heavily 127  
contaminated (Szabó et al. 2007a; Szabó et al. 2007a; 128 Q2  
Szabó et al. 2007b). The recultivation of the sewage 129  
disposal site took place in the spring of 2011. 130  
According to the recultivation plan, the wastewater from 131  
the sewage disposal site was transferred to a sewage- 132  
treatment plant operated by the Debreceni Vízmű Zrt. 133  
(Debrecen Waterworks Ltd.). The sewage sludge was 134  
processed and rendered harmless by the AKSD 135  
Városgazdálkodási Kft. (A.K.S.D. City Management 136  
Ltd. of Debrecen). Based on the recultivation plans, 137  
the pit of the former sandpit—after being cleaned of 138  
wastewater and sewage sludge—was filled with 9000— 139  
9500 m<sup>3</sup> of sand and 2500 m<sup>3</sup> of organic matter rich soil 140  
(Green Side 2008). 141 Q3

2.2 Sampling and Laboratory Tests 142

In order to collect soil and groundwater samples, a total 143  
of 12 shallow groundwater wells have been drilled since 144  
2004 with an Eijkelkamp-type hand auger. Taking the 145  
NE-SW flow direction of the groundwater into 146

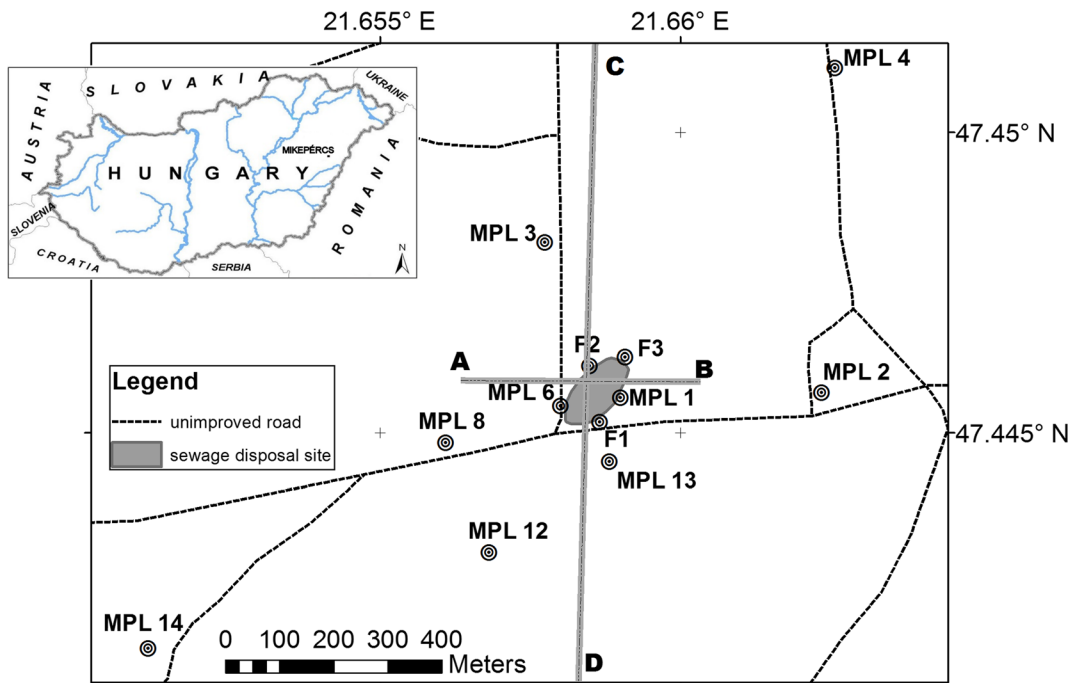


**Fig. 1** The location of the study area, the sampling points, and the vertical sections (A–B, C–D)

147 consideration, the sampling locations (see Fig. 1) were  
 148 assigned so that the samples would provide as much  
 149 information as possible about the groundwater condi-  
 150 tions in the surroundings of the sewage disposal site.  
 151 The well casing was made of PVC pipes with a diameter  
 152 of 50 mm, the lower 1 m section of which is screened.  
 153 This was necessary to prevent the boreholes becoming  
 154 silted up when groundwater flows into the well. The  
 155 bottom depth of the wells was 1 m below the ground-  
 156 water level measured at the time of the installation  
 157 (Table 1).

158 Soil samples were taken from each borehole at every  
 159 20 cm, and were then sealed in plastic bags and trans-  
 160 ferred to the laboratory of the Department of Geology of  
 161 the University of Debrecen. The samples were exsiccated  
 162 at 60 °C, and then their granulometric composition  
 163 was determined by the Köhn-pipette method (Müller  
 164 et al. 2009).

165 For the water sampling a peristaltic pump was used.  
 166 Before sampling we extracted three times the volume of  
 167 water originally contained in the well to obtain water  
 168 from the pore volume. At each sampling time one water  
 169 sample (250 ml) was taken from each well and the depth  
 170 of the groundwater level was measured (Table 1). The  
 171 bubble-free water samples were transferred in tightly  
 172 closed plastic bottles to the Geology Laboratory of the

University of Debrecen, where the Na concentration 173  
 was measured by using a PerkinElmer 3110 AAS. 174

The results of measurements were recorded in a 175  
 Microsoft Excel database. The statistical analyses were 176  
 done using SPSS 20. The maps were edited with the 177  
 Surfer software (version 8.0) (Golden Software LLC), 178  
 by Kriging interpolation. 179

2.3 Model Calculation 180

After the recultivation, we continued the investigation of 181  
 the level of groundwater contamination. Based on the 182  
 test results from three consecutive years after the 183  
 recultivation, no relevant changes in the groundwater 184  
 quality were found. We assume that in the course of the 185  
 three-decade operation of the sewage disposal site both 186  
 the sediment layers and the groundwater itself became 187  
 contaminated to such an extent that the long-term effect 188  
 of the operation must also be taken into consideration. 189

In order to interpret the measurement results and to 190  
 predict the longer-range transport of the contaminants 191  
 via the groundwater, we performed hydrodynamic and 192  
 contaminant transport model calculations. The horizon- 193  
 tal dimension of the modeled area was 1.8 km × 1.4 km 194  
 (2.52 km<sup>2</sup>), whereas its vertical extension reached 115 m 195  
 above the level of the Baltic Sea. The HD72/EOV 196

t1.1  
t1.2  
t1.3  
t1.4  
t1.5  
t1.6  
t1.7  
t1.8  
t1.9  
t1.10  
t1.11  
t1.12  
t1.13  
t1.14  
t1.15

**Table 1** The basic properties of the monitoring wells and main statistical parameters of the depth of groundwater between 2004 and 2014

ID	EOV <i>Y</i>	EOV <i>X</i>	Bottom depth (cm)	Depth of groundwater (cm)			
				Mean	SD	Min.	Max.
MPL1	846942	236792	420	149.8	45.3	57	267
MPL2	847171	236824	370	205.4	10.8	186	224
MPL3	846816	237084	320	238.2	26.1	167	288
MPL4	847191	237425	420	288.1	36.4	171	350
MPL6	846837	236745	420	326.8	24.6	273	366
MPL8	846706	236703	340	256.3	22.7	191	302
MPL12	846758	236518	570	384.3	59.3	301	451
MPL13	846904	236682	400	284.8	40.6	213	360
MPL14	846593	236312	300	193.1	46.2	99	260
F1	846892	236763	534	216.6	44.6	91	269
F2	846874	236844	552	229.7	57.1	131	415
F3	846921	236889	531	339.5	37.1	253	400

EOV Egységes Országos Vetület

coordinate system (EPSG 23700) was applied for the spatial coverages, in which one unit equals 1 m. In order to construct the digital relief map model of the surface, we used the results of our on-site measurements performed by two Trimble S9 dual-frequency, high-precision geodesic GPS instruments. The accuracy of the GPS measurements was 2 cm. The interpolation of the surface was completed with a free triangular mesh.

Based on the analysis of the boring log (Marton 2009) of the confined aquifer well with a bottom depth of 258.6 m in the vicinity of the sewage disposal site, five different geological strata were identified in the model. In the near-surface layers, the dominant fraction of the geological structure is sand; however, 54 m below the surface, 50-m-thick clayey and silty strata appear (Szabó and Szabó 2005; Marton 2009). The determination of the model’s hydrodynamic factors—the diagonal

elements of the hydraulic conductivity tensor ( $K_{xx}$ ,  $K_{yy} \sim 10^{-5} - 10^{-7}$  m/s,  $K_{zz} \sim 10^{-5} - 10^{-8}$  m/s) and the specific storage factor ( $S_s \sim 10^{-5} \text{ m}^{-1}$ )—were based on the particle size distribution of the samples taken from the self-produced shallow groundwater wells, as well as on the data from the confined-aquifer well. For the hydraulic conductivity determination, we have used the Campbell formula:

$$K = 4 \times 10^{-5} \times e^{-6.9f_{\text{clay}} - 3.7f_{\text{silt}}}$$

where  $f_{\text{clay}}$  and  $f_{\text{silt}}$  are the clay and silt fractions, respectively (Campbell 1985).

Figure 2 shows the grain size distributions along the section of three selected monitoring wells (MPL1, MPL2, MPL3). All the other wells show similar distribution. The graphs show that the dominant fraction is

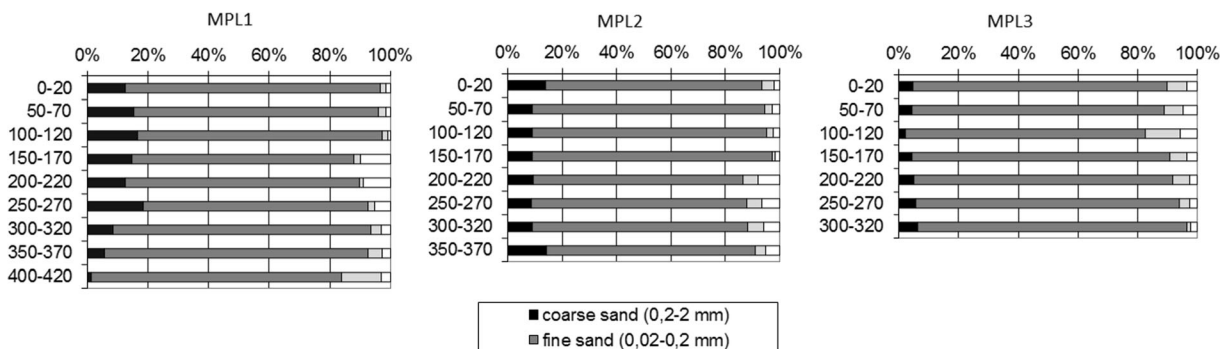


**Fig. 2** The grain size distributions of the MPL1, MPL2, and MPL3 wells



229 fine sand (over 80 %) and the fraction of coarse sand  
 230 falls below 20 %. The sum of the fractions of silt and  
 231 clay, which essentially determines the hydraulic conduc-  
 232 tivity, remains below 20 % in each layer of each well.

233 In order to calibrate the system’s hydrodynamic pa-  
 234 rameters, we first made temporally varying hydrody-  
 235 namic model calculations. This was possible because  
 236 the required set of rainfall and evapotranspiration input  
 237 data for 3 years after the recultivation of the disposal site  
 238 was available, as were the results of the hydrodynamic  
 239 piezometry measurements necessary for the calibration  
 240 and validation of the model. During the process of  
 241 modeling, we solved Eq. (1):

$$\frac{\partial}{\partial x} \left( K_{xx} \frac{\partial h}{\partial x} \right) + \frac{\partial}{\partial y} \left( K_{yy} \frac{\partial h}{\partial y} \right) + \frac{\partial}{\partial z} \left( K_{zz} \frac{\partial h}{\partial z} \right) - w = S_s \frac{\partial h}{\partial t} \quad (1)$$

Q6 242 where  $w$  is the volumetric flux per unit volume  
 243 representing the sources and sinks of water and  $h$  is  
 244 the hydraulic head. During the transient calculations,  
 245 the hydrodynamic potential values at the circumference  
 246 of the sampling area were set so that they would ap-  
 247 proximate the water levels measured in the monitoring  
 248 wells closest to the edge of the area (ID: MPL-4 and  
 249 MPL-14) as much as possible. The hydrodynamic model  
 250 was run by the USGS MODFLOW 2005 numerical  
 251 engine (Harbaugh 2005). Figure 3 shows the input  
 252 infiltration and evapotranspiration data of the time-  
 253 dependent model calculations, as well as the calculated  
 254

255 results of the hydrodynamic potential, in comparison  
 256 with the measured data from a few selected monitoring  
 257 wells.

258 In the course of the calibration, three of the studied  
 259 model parameters—the infiltrated percentage of total  
 260 rainfall, the average rate of evapotranspiration, and the  
 261 hydraulic conductivity of the second stratum—were set  
 262 in such a way that in the other monitoring wells the sum  
 263 of root-mean-squares (RMS) of the measured and cal-  
 264 culated water levels—averaged to all sampling times—  
 265 were as low as possible. In Fig. 4 a calibration curve  
 266 relating to a sampling time (day 446), which is selected  
 267 as an example, shows that the normalized RMS value is  
 268 quite low (6 %) and the correlation coefficient approx-  
 269 imates 1 ( $r=0.966$ ). Thus, the model can be considered  
 270 reliable.

271 We created the steady-state hydrodynamic model  
 272 using the optimized parameters of the transient model  
 273 and the average annual infiltration typical of the area.  
 274 The solution of the steady-state model was used in the  
 275 contaminant transport calculations.

276 For the contaminant transport calculations, sodium  
 277 was chosen because of its low retardation factor ( $R \sim 1.5$ ) (Rowe et al. 2004); i.e., it is relatively con-  
 278 servative, so it does not transmute during transport via  
 279 groundwater, and it is poorly adsorbed (Greenwood and  
 280 Earnshaw 1999; Sayyed and Bhosle 2011).  
 281 Another important condition was that the given contam-  
 282 inant should originate primarily from the wastewater  
 283

**Fig. 3** The input infiltration and evapotranspiration data of the transient model calculations and the calculated hydrodynamic potentials (continuous curves), with the water levels measured in the monitoring wells

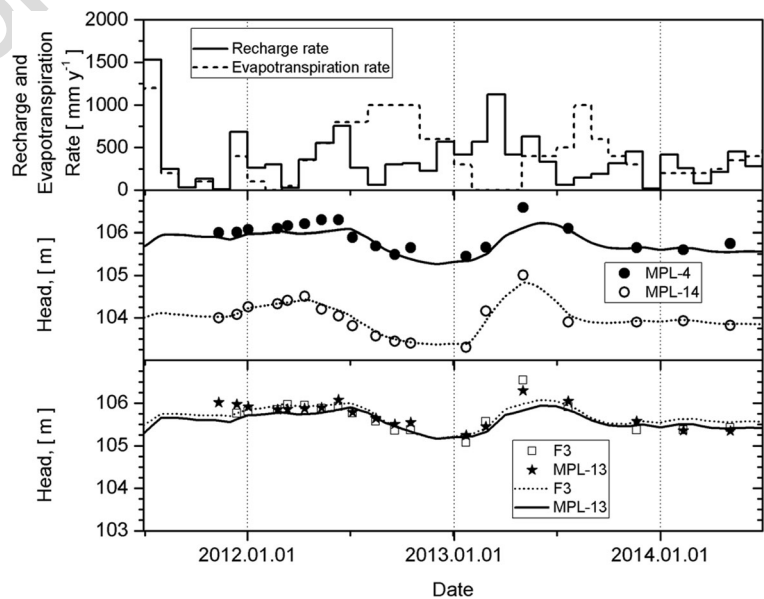
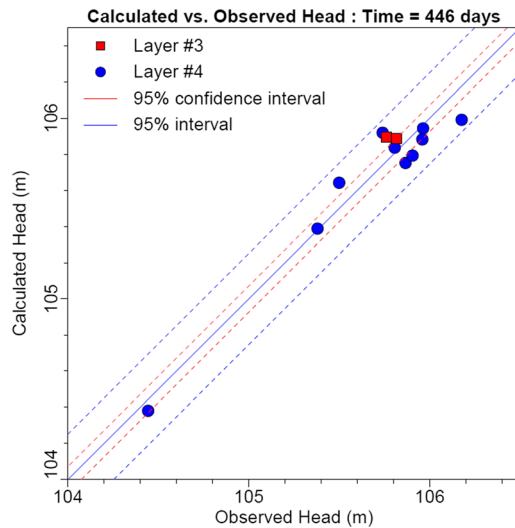




**Fig. 4** One calibration curve (relating to day 446 of sampling) of the transient hydrodynamic model



Num. of Data Points : 12  
 Standard Error of the Estimate : 0.033 (m)  
 Root Mean Squared : 0.111 (m)  
 Normalized RMS : 6.395 ( % )  
 Correlation Coefficient : 0.966  
 Max. Residual: -0.186 (m) at MPL-4/1  
 Min. Residual: 0.007 (m) at MPL-12/1  
 Residual Mean : -0.001 (m)  
 Abs. Residual Mean : 0.095 (m)

284 collected from the disposal site. When modeling the  
 285 contaminant transport, we used Eq. (2):

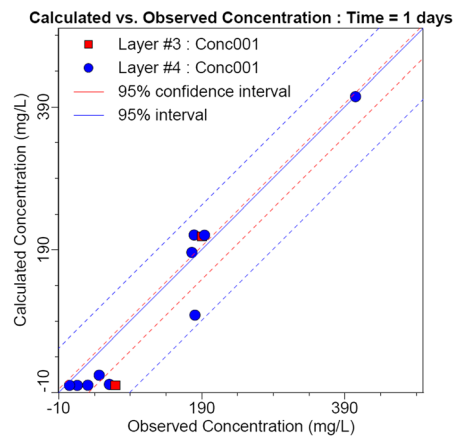
$$\frac{\partial(\theta C)}{\partial t} = \frac{\partial}{\partial x_i} \left( \theta D_{ij} \frac{\partial C}{\partial x_j} \right) - \frac{\partial}{\partial x_i} (\theta v_i C) \quad (2)$$

286 where  $C$  is the dissolved concentration of sodium;  $\theta$  is the  
 288 porosity of the subsurface medium;  $t$  is time;  $x_i$  is the  
 289 distance along the respective Cartesian coordinate axis;  
 290  $D_{ij}$  is the hydrodynamic dispersion coefficient tensor; and  
 291  $v_i$  is the Darcy velocity, which can be determined from the

solution of Eq. (1). We determined the diffusion constant  
 that influences the contaminant transport as the molecular  
 diffusion coefficient of sodium in water:  $4 \times 10^{-9} \text{ m}^2/\text{s}$ .  
 The longitudinal, horizontal, and vertical dispersivities  
 were specified as 10, 1, and 0.1 m, respectively.

To calculate the contaminant transport, the  
 MT3DMS v. 5.2 numerical transport engine (Zheng  
 and Wang 1999) was applied. In the course of the model  
 calibration, the parameters to be fitted were the Na  
 concentrations in the northern and southern volumes of  
 the disposal site. The transport calculations (Fig. 5)

**Fig. 5** The calibration curve of the transport calculations



Num. of Data Points : 12  
 Standard Error of the Estimate : 10.687 (mg/L)  
 Root Mean Squared : 40.043 (mg/L)  
 Normalized RMS : 10.013 ( % )  
 Correlation Coefficient : 0.965  
 Max. Residual: -82.886 (mg/L) at MPL-13/A  
 Min. Residual: -1.156 (mg/L) at MPL-6/A  
 Residual Mean : -18.632 (mg/L)  
 Abs. Residual Mean : 31.134 (mg/L)

303 were calibrated to the sampling time following  
 304 recultivation, for which reliable measurement data  
 305 were available. Based on the graph it can be  
 306 established that the reliability of the transport model  
 307 is acceptable, since the normalized RMS is around  
 308 10 % and the value of the correlation coefficient  
 309 ( $r=0.965$ ) approximates to 1.

### 310 3 Results and Discussion

311 In the first stage we had to verify that sodium is also  
 312 suitable for the calibration of the contaminant trans-  
 313 port model in the sense that it originates primarily  
 314 from the wastewater deposited at the disposal site  
 315 (Szabó and Bessenyei 2013). This is because in al-  
 316 kaline soils the sodium contents of the groundwater  
 317 may increase under natural conditions as well.  
 318 However, based on the test results of the water sam-  
 319 ples originating from the monitoring wells, it can be  
 320 clearly established that in the affected area of the  
 321 sewage deposit it is not necessary to take into account  
 322 any alkaline-formation process, since in the wells  
 323 located further away from the disposal site (MPL14,  
 324 MPL2, MPL4) we consistently measured quite low  
 325 (under 20 mg/l) sodium content. Values greater by  
 326 about one order of magnitude (150–500 mg/l) were  
 327 found without exception in the wells in the immedi-  
 328 ate vicinity of the sewage disposal site (MPL6, F2,  
 329 MPL1, F1, F3, MPL13) (see Figs. 1 and 6).

330 Regarding sodium transport, we used the model to  
 331 investigate two consecutive time periods. For the first  
 332 period we assumed a disposal site that had been contin-  
 333 uously operational for three decades and filled with

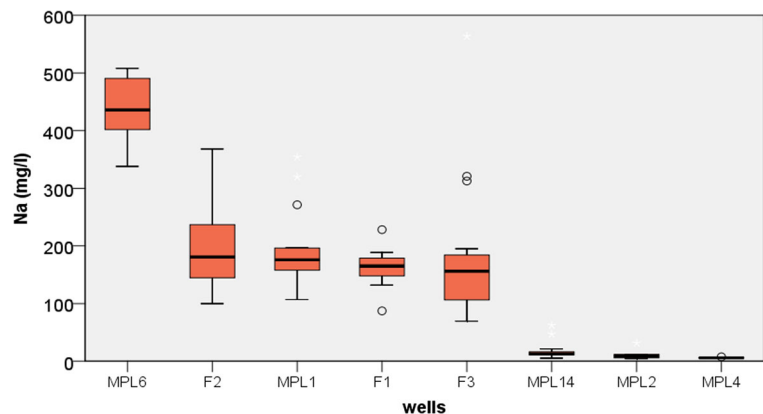
334 contaminants. The second period refers to the disposal  
 335 site that had been recultivated and filled with sand after  
 336 the removal of the contaminants.

337 In the 30-year operational period, the hydrodynamic  
 338 potential field was calculated for the static condition,  
 339 with the important difference in comparison to the tran-  
 340 sient model that in the area of the disposal site we  
 341 specified the water level that was available based on  
 342 the measurement data from the operational period (see  
 343 Fig. 7a).

344 In the operational period, at the border of the  
 345 saturated and unsaturated zones, the maximal hori-  
 346 zontal infiltration speed—according to calculations  
 347 based on the model—was  $4.2 \times 10^{-6}$  m/s, whereas  
 348 the maximal vertical infiltration speed was lower, at  
 349  $3.1 \times 10^{-6}$  m/s in areas close to the sewage disposal  
 350 site (Fig. 7a). In the period following recultivation, in  
 351 both the horizontal ( $1.3 \times 10^{-6}$  m/s) and the vertical  
 352 ( $9.2 \times 10^{-7}$  m/s) infiltration speed, a certain decrease  
 353 was detected, which can be explained by the cessa-  
 354 tion of the dome-like hydrodynamic potential field  
 355 that came about as a consequence of the sewage  
 356 disposal (Fig. 7b).

357 When simulating the contaminant transport, in the  
 358 dome-like potential field typical of the operational  
 359 period, in the northeastern 3/4 and southwestern 1/4  
 360 volumes of the disposal site, constant sodium con-  
 361 centrations of 200 and 500 mg/l were assumed, re-  
 362 spectively. The sewage disposal was divided into two  
 363 parts by an earth bank, and the two catch basin parts  
 364 became isolated from each other whenever the water  
 365 levels were low; therefore, in the southwestern basin  
 366 part increased evaporation could occur, which result-  
 367 ed in an increase in the Na concentration (Fig. 8a).

**Fig. 6** The sodium contents of the water from shallow groundwater wells, based on the measurements performed during the study period (2004–2014). The extreme values (third quartile [Q3] + 3 interquartile range [IQR]) were not plotted in the graph



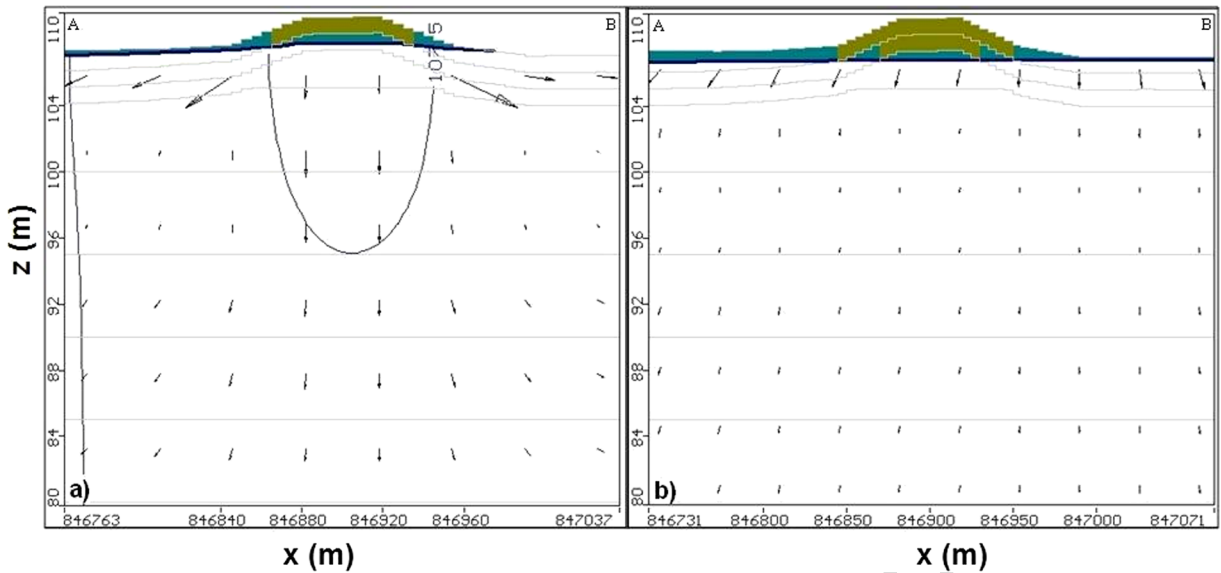


**Fig. 7** **a** The W-E orientated vertical picture of the dome-like hydrodynamic potential field in the course of operation. **b** The W-E orientated vertical picture of the hydrodynamic potential field after recultivation

368 The wastewater had been disposed in the larger,  
 369 northeastern basin part. Consequently, the possibility  
 370 of a continuous thinning was present.

During the functional period, in the groundwater 371  
 dome that was being formed by the disposed wastewater, 372  
 a radial transport of contamination can be observed; 373

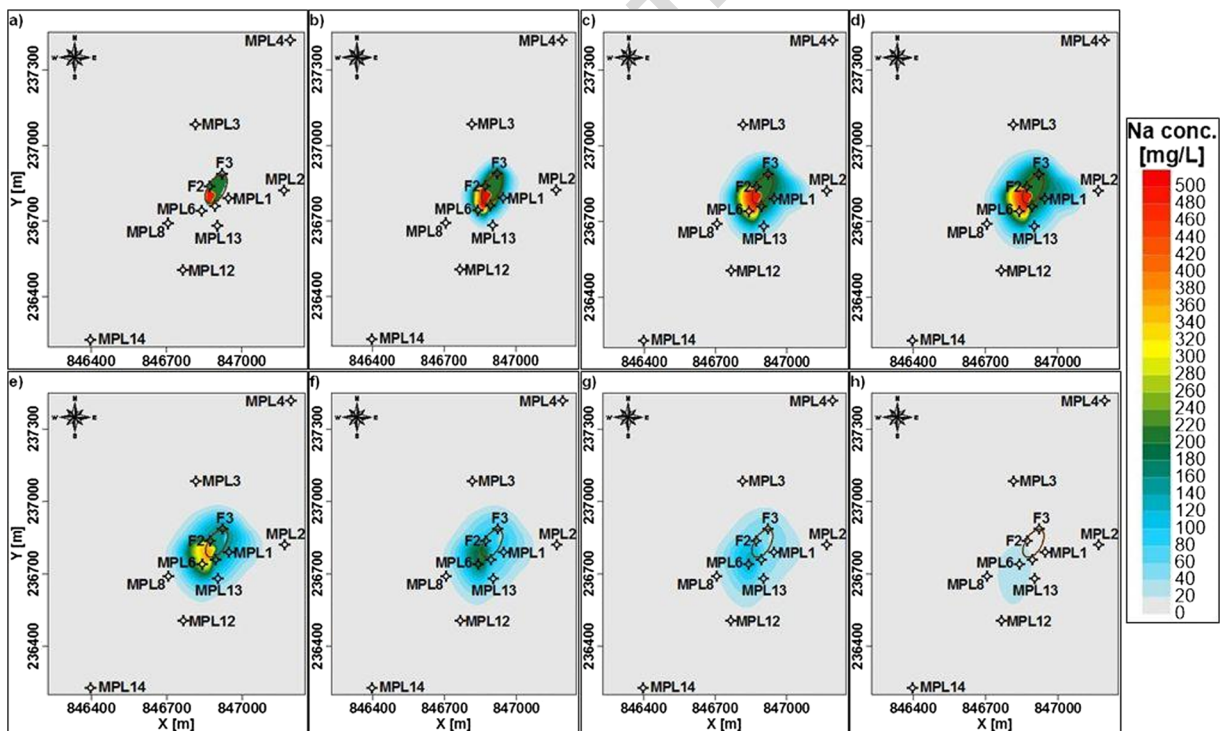


**Fig. 8** The horizontal transport of Na contamination, 3 m below the surface: **a** the beginning of operation (1982); **b** 1st year of operation (1983); **c** 10th year of operation (1992); **d** end of

operation, recultivation (2011); **e** 1st year after recultivation (2012); **f** 5th year after recultivation (2016); **g** 10th year after recultivation (2021); and **h** 30th year after recultivation (2041)

374 therefore, the NE-SW flow direction, which is charac- 423  
375 teristic under natural conditions, was hindered. The 424  
376 height of the groundwater dome in the surrounding areas 425  
377 exceeded the average natural groundwater level by 1 m 426  
378 on average. According to our calculations, the contam- 427  
379 ination transport at a depth of 3 m reached a distance of 428  
380 50–100 m by the end of the first year of contamination 429  
381 (Fig. 8b). At such distances the Na concentration de- 430  
382 creased to the level of the background concentration 431  
383 level (20 mg/l) typical of the area. After 30 years had 432  
384 passed (by the end of the operational period), at such a 433  
385 depth below the surface the Na contamination—accord- 434  
386 ing to both the model calculations and the test results of 435  
387 the collected water samples—could be detected at a 436  
388 distance of up to 200 m, and the size of the affected 437  
389 contamination area was 112,000 m<sup>2</sup> (Fig. 8d). Sodium is 438  
390 a conservative, i.e., enduring, contaminant, and its rate 439  
391 of release from the sewage disposal site is more or less 440  
392 time-independent; therefore, the limited horizontal di- 441  
393 mension of the contamination suggests that in the near- 442  
394 surface layers the vertical component must be given 443  
395 greater emphasis in the transport process. 444

396 In the calculations for the 30-year period after 445  
397 recultivation, the starting contaminant concentration 446  
398 was borrowed from the concentration distribution re- 447  
399 sults of the end of the first period, except for the volume 448  
400 size of the disposal site itself, where we defined a clean, 449  
401 contaminant-free territory filled with sand, since in the 450  
402 course of recultivation both the wastewater and the 451  
403 sewage sludge were removed from the disposal site 452  
404 and the cleaned pit was filled with pure sand. With these 453  
405 results we predicted the horizontal transport of the con- 454  
406 taminants for 30 years. In this period the natural, the NE- 455  
407 SW groundwater flow direction already prevails. Since 456  
408 the resupply of contaminants has ceased, the model 457  
409 predicts the gradual decrease in the Na concentration. 458  
410 Based on the model simulations, after a year a 350– 459  
411 400 mg/l Na concentration can still be expected in the 460  
412 southwestern corner of the disposal site (Fig. 8e). This 461  
413 result is further supported by the 393.3 mg/l concentra- 462  
414 tion value measured in the MP6 monitoring well in 463  
415 July 2012. According to the model, in the fifth year after 464  
416 recultivation the Na concentration would decrease to 465  
417 250–300 mg/l (Fig. 8f), and in 10 years' time in the 466  
418 southwestern corner of the sewage disposal site the 467  
419 model predicts a mere 140–160 mg/l concentration 468  
420 (Fig. 8g). The model indicates that after 30 years have 469  
421 passed, in the areas surrounding the above-mentioned 470  
422 location, in a 26,000 m<sup>2</sup> area this value (20–40 mg/l) 471

will still exceed the limit values to a certain extent, but 423  
apart from this, we can base our calculations on concen- 424  
trations below 20 mg/l, even for the former sewage 425  
disposal site itself. In other words, during the 30-year 426  
period following recultivation, the size of the contami- 427  
nated area would gradually decrease and also slowly 428  
migrate in a SW direction (Fig. 8h). 429

In addition to its horizontal transport, the vertical 430  
distribution of the contamination was also modeled. 431  
Figure 9a–d demonstrates the outcome of the vertical 432  
transport of the contamination, in the 30-year time span 433  
from the start of operation as a functional sewage dis- 434  
posal site to the beginning of its recultivation. It can be 435  
clearly seen that the contamination already approaches 436  
the 54-m-deep water-impermeable layer in the first year 437  
(Fig. 9b). At such a depth the vertical transport of the 438  
contaminants slows down, and by the end of the oper- 439  
ational period (i.e., in the 30th year following the start of 440  
its functioning) it reaches down to about 70 m (Fig. 9d). 441  
The highest Na concentrations can be detected under the 442  
south basin part of the sewage disposal site, due to the 443  
concentration by evaporation mentioned earlier. 444  
Concentrations higher than 400 mg/l were undetectable 445  
40 m below the surface. It is also clearly observable that 446  
because of the continuous contaminant resupply and the 447  
water-impermeable layer found at a depth of 54 m, 448  
about 50 m below the surface a more intensive horizon- 449  
tal spread has developed. In this zone, the polluted water 450  
can reach distances as great as 400 m, which signifi- 451  
cantly exceeds those calculated for near-surface layers. 452  
The horizontal transport is more intensive toward the S- 453  
SW, since this fits the local groundwater flow direction. 454

In the first year after recultivation, no significant 455  
changes were observed. However, as Fig. 9e clearly 456  
shows, the contamination rate significantly decreased 457  
in the near-surface layers; i.e., the 400–500 mg/l Na 458  
concentration was detected only in a much narrower 459  
strip. In the 5 years after recultivation, the Na concen- 460  
tration reduces to below 300 mg/l in the near-surface 461  
layers even in the most heavily contaminated parts. 462  
However, in the zone lying between 30 and 40 m below 463  
the surface, below the southern basin of the sewage 464  
disposal site, the model still indicates a value of 465  
350 mg/l (Fig. 9f). After 10 years, the contamination 466  
decreased further: the highest concentration was 467  
290 mg/l, which appeared at greater depth, between 35 468  
and 55 m below the surface (Fig. 9g). In the 30th year 469  
following recultivation, some contamination can still be 470  
detected, but its level never exceeds 210 mg/l. The most 471

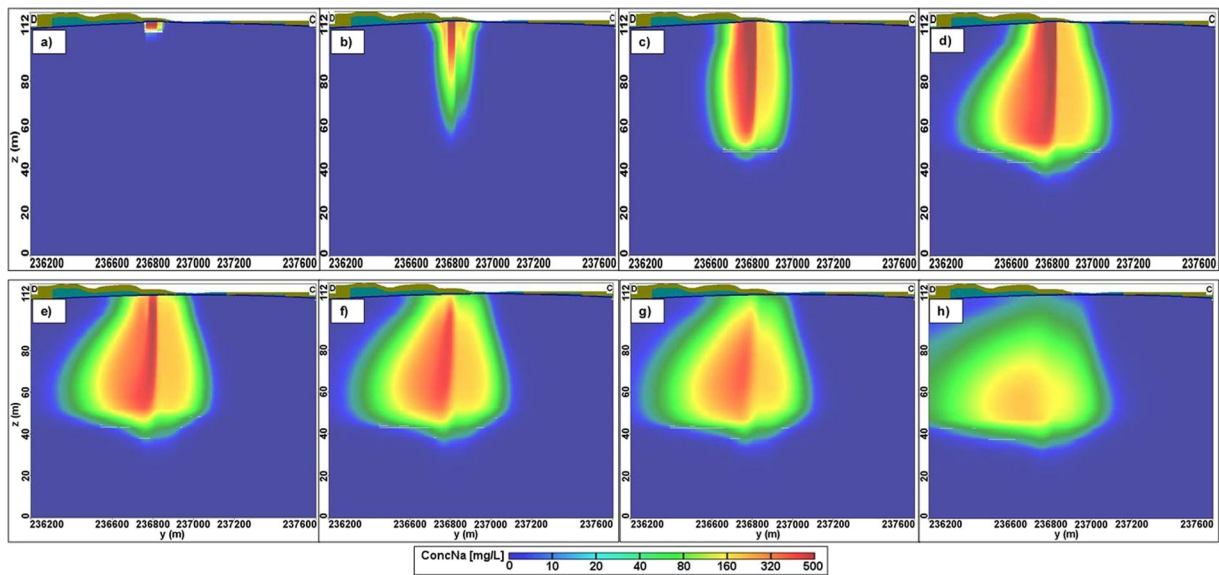


**Fig. 9** The vertical transport of contamination: **a** the beginning of operation (1982); **b** 1st year of operation (1987); **c** 10th year of operation (1992); **d** end of operation, recultivation (2011); **e** 1st

year after recultivation (2012); **f** 5th year after recultivation (2016); **g** 10th year after recultivation (2021); and **h** 30th year after recultivation (2041)

472 heavily polluted zone shifted deeper, appearing in the  
 473 strip 50–60 m below the surface. However, in the near-  
 474 surface layers, these values fell to around or below the  
 475 background concentrations (Fig. 9h).

476 The migration of the contamination in a S-SW direc-  
 477 tion was considerable even in the period after  
 478 recultivation. The infiltration continued to be most in-  
 479 tensive above the water-impermeable layer that runs  
 480 54 m below the surface. After 10 years, water with a

481 higher than 20 mg/l Na concentration reached as far as  
 482 about 500 m (Fig. 9g). Unfortunately, based on this  
 483 model, we could not establish precisely how far the  
 484 contaminated water may travel in 30 years, because  
 485 the size of the modeled area does not allow this.  
 486 However, we can assume that the distance covered  
 487 may be somewhere around 600–700 m. Although the  
 488 dominant transport direction is S-SW, due to diffusion  
 489 the contamination can spread toward the north as well.

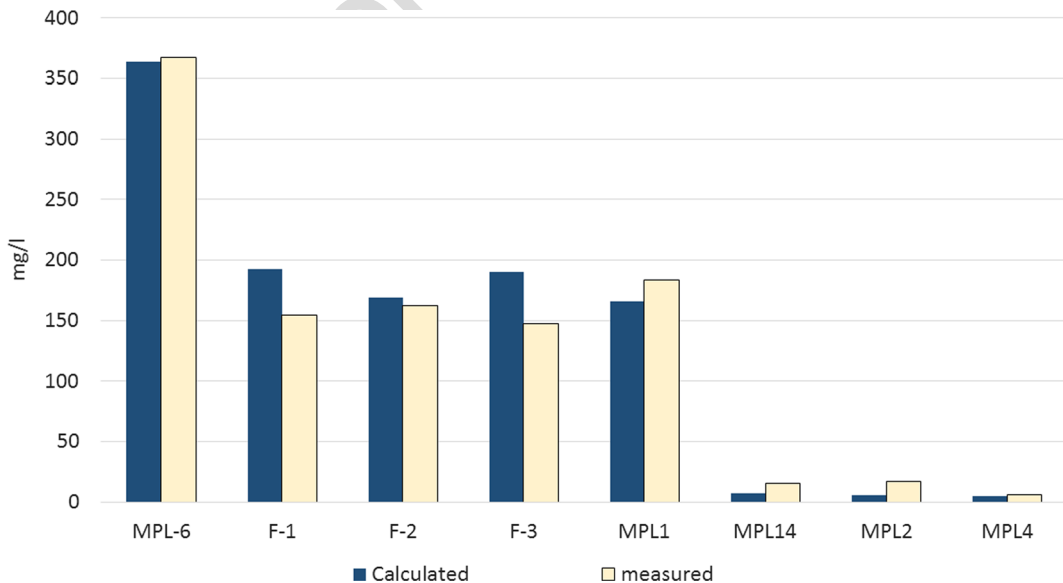


**Fig. 10** The measured and the calculated values for the first year after the recultivation



490 However, the rate of this process is a mere 7 m per  
491 30 years. The water-impermeable layer considerably  
492 hindered and slowed down the vertical transport of  
493 contaminants, but during the 30 years following  
494 recultivation, the contamination reached a further 6 m  
495 down (i.e., 76 m below the surface).

496 In order to verify the reliability of our model, we  
497 compared our measured results in the first year after the  
498 recultivation to the calculated values of the model for  
499 the end of the first year after the recultivation. In Fig. 10  
500 it can be seen that the calculated values correspond with  
501 the measured ones, even though some differences may  
502 occur because of the uncertainty of the sampling and  
503 laboratory measurements as well as the model  
504 calculation.

#### 505 4 Conclusions

506 In the present study we suggested a novel calibration  
507 method of the model for hydrodynamic and contami-  
508 nant transport, shown via the example of a sewage  
509 disposal site set up uninsulated in a sandy environment.  
510 In the case of the hydrodynamic model, we applied  
511 time-dependent model calculations in order to fit the  
512 individual hydrodynamic parameters. For the calibra-  
513 tion of the transport model, sodium—which has a neg-  
514 ligible retardation factor—was used.

515 We proved that the Na content of the groundwater—  
516 which exceeded the 20 mg/l background concentration  
517 and close to the disposal site even reached 500 mg/l—  
518 definitely originated from the sewage disposal site.  
519 Consequently, sodium—due to its low retardation fac-  
520 tor—proved to be a suitable element to allow us to  
521 estimate and predict the maximal spatial extension of  
522 the contamination. We established that by the end of the  
523 operational period the polluting effect of the sewage  
524 disposal site remained detectable within a 200-m range  
525 in the near-surface (1–3 m deep) layers, which is equiv-  
526 alent to an area slightly greater than 0.1 km<sup>2</sup>. However,  
527 40–50 m below the surface, the contaminated area is  
528 substantially—at least three times—greater than that  
529 measured near the surface. After recultivation the resup-  
530 ply of contamination ceased and according to the model,  
531 by the end of the modeled period the size of the polluted  
532 area would diminish to one-fifth in the near-surface  
533 layers and the Na concentration would decrease approx-  
534 imately to the level of the background concentration.  
535 However, in the deeper layers (40–50 m below surface)

the Na concentration would still remain higher by about 536  
one order of magnitude. 537

In this pilot study we have shown that the reliability 538  
of contamination transport model for a sewage disposal 539  
site can be justified. The developed model calibration 540  
method can be profitably applied to similar relatively 541  
small-scale sites to estimate the maximal spatial exten- 542  
sion of contamination in a sedimentary environment, 543  
and it may provide a proper basis for modeling the 544  
transport of polluting agents that are present in similar 545  
sewage disposal sites, which may pose a significantly 546  
higher risk in terms of human health and safety. 547

**Acknowledgments** This research was realized in the framework 550  
of TÁMOP 4.2.4. A/2-11-1-2012-0001 “National Excellence 551  
Program—Designing and Operating a Personal Support System 552  
Convergence Program for Hungarian Students and Researchers,” 553  
and it was supported by TÁMOP-4.2.2/B-10/1-2010-0024 as well. 554  
The project was cofinanced by the European Union and European 555  
Social Fund. 556  
557

#### References 558

- Al-Khashman, O. A. (2008). Assessment of the spring water 560  
quality in The Shoubak area, Jordan. *Environmentalist*, 28,  
203–215. 561  
562  
Campbell, C. S. (1985). *Soil Physics with Basic*. New York: 563  
Elsevier. 564  
Chakraborty, R., & Ghosh, A. (2009). Finite difference method for 565  
computation of sodium and chloride migration in porous 566  
media, Proceedings of the Indian Geotechnical Conference, 567  
pp. 268–271. 568  
Chawla, A., & Singh, S. K. (2014). Modelling of contaminant 569  
transport from landfills. *International Journal of Engineering*  
*Science and Innovative Technology*, 3(5), 222–227. 570  
571  
Cho, J.-C., Cho, H. B., & Kim, S.-J. (2000). Heavy contamination 572  
of a subsurface aquifer and a stream by livestock wastewater 573  
in a stock farming area, Wonju, Korea. *Environmental*  
*Pollution*, 109, 137–146. 574  
575  
Datta, B., Chakraborty, D., & Dhar, A. (2011). Identification of 576  
unknown groundwater pollution sources using classical op- 577  
timization with linked simulation. *Journal of Hydro-*  
*Environment Research*, 5, 25–36. 578  
579  
Delkash, M., Al-Faraj, F. A. M., & Scholz, M. (2014). Comparing 580  
the export coefficient approach with the soil and water as- 581  
sessment tool to predict phosphorous pollution: the Kan 582  
watershed case study. *Water, Air, and Soil Pollution*, 225,  
2122. 583  
584  
Dövényi, Z. (Ed.). (2010). *Magyarország kistájainak katasztere*  
*(Inventory of natural micro-regions of Hungary)*. Budapest: 585  
MTA FKI. 586  
587  
Fejes, I., Farsang, A., & Puskás, I. (2012). Potential effects of the 588  
contaminated groundwater on human health in Szeged, SE 589

- 590 Hungary. *Carpathian Journal of Earth and Environmental*  
591 *Sciences*, 7(3), 119–126.
- 592 Green Side, K. (2008). *Mikepércs külterület 080 hrsz. alatti*  
593 *települési folyékony hulladék leürítőhely rekultivációja.*  
594 *(The recultivation of the sewage disposal site at 080 Hrsz.*  
595 *in the outskirts of Mikepércs. Plan documentation.)*. Miskolc:  
596 Tervdokumentáció.
- 597 Greenwood, N. N., & Earnshaw, A. (1999). *Az elemek kémiája I.*  
598 *(Chemistry of elements I.)*. Budapest: Nemzeti  
599 Tankönyvkiadó.
- 600 Harbaugh, A. W. (2005). MODFLOW-2005, the U.S. Geological  
601 Survey modular ground-water model—the ground-water  
602 flow process: U.S. Geological Survey Techniques and  
603 Methods 6-A16.
- 604 Kerényi, A. (2003). *Európa Természet- és Környezetvédelme*  
605 *(Nature- and environmental protection of Europe)*.  
606 Budapest: Nemzeti Tankönyv Kiadó Rt.
- 607 Marton, L. (2009). *Energiaszint változások az ÉK-Alföld fő vízadó*  
608 *rétegeiben. (Energy level changes in the main water-*  
609 *supplying ground layers in the north-eastern region of the*  
610 *Great Hungarian Plain.)* (pp. 1–2). Debrecen: Debreceni  
611 műszaki közlemények.
- Q7 612 MSZ 14043/3-79 Hungarian Standard. Soil mechanical studies—  
613 determination of particle size of soils. Talajmechanikai  
614 vizsgálatok—Szemeloszlás meghatározása
- 615 Müller, H. W., Dohrmann, R., Klosa, D., Rehder, S., &  
616 Eckelmann, W. W. (2009). Comparison of two procedures  
617 for particle-size analysis: Köhn pipette and X-ray  
618 granulometry. *Journal of Plant Nutrition and Soil Science*,  
619 172(2), 172–179.
- 620 Nakaya, S., Natsume, H., Masuda, H., Mitamura, M., Biswas,  
621 D. K., & Seddique, A. A. (2011). Effect of groundwater  
622 flow on forming arsenic contaminated groundwater in  
623 Sonargaon, Bangladesh. *Journal of Hydrology*, 409,  
624 724–736.
- Q8 625 Ozdemir, A. (2011). Using a binary logistic regression method and  
626 GIS for evaluating and mapping the groundwater spring  
627 potential in the Sultan Mountains (Aksehir, Turkey).  
628 *Journal of Hydrology*, 405, 123–136.
- 629 Panno, S. V., Hackley, K. C., Hwang, H. H., Greenberg, S.,  
630 Krapac, I. G., Landsberger, S., & O’Kelly, D. J. (2002).  
631 Source identification of sodium and chloride contamination  
632 in natural waters: preliminary results. In *12th Annual*  
633 *Research Conference of the Illinois Groundwater*  
634 *Consortium. Research on Agrichemicals in Illinois*.  
635 Carbondale, Illinois: Groundwater Status and Future  
636 Direction XII.
- 637 Panno, S. V., Hackley, K. C., Hwang, H. H., Greenberg, S. E.,  
638 Krapac, I. G., Landsberger, S., & O’Kelly, D. J. (2006).  
639 Characterization and identification of Na-Cl sources in  
640 ground water. *Groundwater*, 44(2), 176–187.
- 641 Phan, K., Phan, S., Heng, S., Huoy, L., & Kim, K.-W. (2014).  
642 Assessing arsenic intake from groundwater and rice by resi-  
643 dents in Prey Veng province, Cambodia. *Environmental*  
644 *Pollution*, 185, 84–89.
- 645 Phan, K., Phan, S., Huoy, L., Suy, B., Wong, M. H., Hashim, J. H.,  
646 Yasin, M. S. M., Aljunid, S. M., Sthiannopkao, S., & Kim,  
647 K.-W. (2013). Assessing mixed trace elements in groundwa-  
648 ter and their health risk of residents living in the Mekong  
649 River basin of Cambodia. *Environmental Pollution*, 182,  
650 111–119.
- Regadio, M., Ruiz, A. I., de Soto, I. S., Rastroero, M. R., Sánchez,  
651 N., Gismera, M. J., Sevilla, M. T., da Silva, P., Procopio, R.  
652 J., & Cuevas, J. (2011). Pollution profiles and physicochem-  
653 ical parameters in old uncontrolled landfills. *Waste*  
654 *Management*, 32, 482–497.
- 655 Rowe, R. K., Quigley, R. M., Brachman, R. W. I., & Booker, J. R.  
656 (2004). *Barrier system for waste disposal facilities*. London:  
657 Taylor and Francis.
- 658 Sayyed, A. J., & Bhosle, B. A. (2011). Analysis of chloride,  
659 sodium and potassium in groundwater samples of Nanded  
660 City in Mahabharata, India. *European Journal of*  
661 *Experimental Biology*, 1(1), 74–82.
- 662 Shahid, S., Nath, S. K., & Roy, J. (2000). Groundwater potential  
663 modelling in a soft rock area using a GIS. *International*  
664 *Journal of Remote Sensing*, 21(9), 1919–1924.
- 665 Sipos, P., Kovács Kis, V., Márton, E., Németh, T., May, Z., &  
666 Szalai, Z. (2012). Lead and zinc in the suspended particulate  
667 matter and settled dust in Budapest, Hungary. *European*  
668 *Chemical Bulletin*, 1(11), 449–454.
- 669 Slack, R. J., Gronow, J. R., Hall, D. H., & Voulvoulis, N. (2007).  
670 Household hazardous waste disposal to landfill: using  
671 LandSim to model leachate migration. *Environmental*  
672 *Pollution*, 146, 501–509.
- 673 Slack, R. J., Gronow, J. R., & Voulvoulis, N. (2005).  
674 Household hazardous waste in municipal landfills: con-  
675 taminants in leachate. *Science of the Total Environment*,  
676 337, 119–137.
- 677 Somlyódi, L. (2002). A hazai vízgazdálkodás és stratégiai pillérei.  
678 In L. Somlyódi (Ed.), *A hazai vízgazdálkodás stratégiai*  
679 *kérdései. (Strategic issues of national water management.)*  
680 (pp. 23–74). Budapest: MTA.
- 681 Sonneveld, M. P. W., Brus, D. J., & Roelsma, J. (2010). Validation  
682 of regression models for nitrate concentrations in the upper  
683 groundwater in sandy soils. *Environmental Pollution*, 158,  
684 92–97.
- 685 Szabó, Gy., & Bessenyei, É. (2013). Studying groundwater pollu-  
686 tion in the surroundings of a recultivated sewage disposal site  
687 in eastern Hungary. *Journal of Selçuk University Natural and*  
688 *Applied Science, Special Issue (I) 1–12*.
- 689 Szabó, S., Papp, L., & Szabó, G. (2007a). Investigation of a  
690 communal sewage disposal site from the aspect of landscape  
691 protection. In M. Boltíziar (Ed.), *Implementation of land-*  
692 *scape ecology in new and changing conditions* (pp. 415–  
693 420). Bratislava: ILE Slovak Academy of Sciences.
- 694 Szabó, S., & Szabó, G. (2005). *Mikepércs községi folyékony*  
695 *hulladék leürítőhely részleges környezetvédelmi*  
696 *felülvizsgálata*. Debrecen: (Partial environmental review of  
697 the municipal sewage disposal site of Mikepércs town.)  
698 manuscript.
- 699 Szabó, S., Szabó, G., Fodor, C., & Papp, L. (2007b). Sewage  
700 disposal and its effects on groundwater and soil quality. In  
701 E. Kallabova, B. Frantal, & P. Klusacek (Eds.), *Regions,*  
702 *localities and landscapes in new Europe*. Brno,  
703 Czech Republic: 7th International Geographical  
704 Conference CONGEO’07, Enhanced Abstracts and Full  
705 Texts.
- 706 Szabó, G., Szabó, S., Szabó, A., & Szemán, B. (2007c).  
707 Spatial and time variations of the groundwater quality of  
708 two different landscapes. In M. Boltíziar (Ed.),  
709 *Implementation of landscape ecology in new and*  
710



- 711 *changing conditions* (pp. 421–427). Bratislava: ILE 720  
712 Slovak Academy of Sciences. 721
- 713 Zhan, T. L. T., Guan, C., Xie, H. J., & Chena, Y. M. (2013). 722  
714 Vertical migration of leachate pollutants in clayey soils be- 723  
715 neath an uncontrolled landfill at Huainan, China: a field and 724  
716 theoretical investigation. *Science of the Total Environment*, 725  
717 *470–471*, 290–298. 726
- 718 Zhang, H., Xu, W. L., & Hiscock, K. M. (2013). Application of 727  
719 MT3DMS and geographic information system to evaluation  
728 of groundwater contamination in the Sherwood Sandstone  
Aquifer, UK. *Water, Air, and Soil Pollution*, *224*, 1438.
- Zheng, C., & Wang, P. P. (1999). *MT3DMS: a modular three-  
dimensional multispecies transport model for simulation of  
advection, dispersion and chemical reactions of contami-  
nants in groundwater systems; documentation and user's  
guide*, Contract Report SERDP-99-1. Vicksburg, MS: U.S.  
Army Engineer Research and Development Center.

UNCORRECTED PROOF

## AUTHOR QUERIES

### AUTHOR PLEASE ANSWER ALL QUERIES.

- Q1. Please check captured article title, if appropriate.
- Q2. Szabó et al. 2007 has been changed to Szabó et al. 2007a as per the reference list. Please check if okay.
- Q3. Green Side Kft. 2008 has been changed to Green Side 2008 as per the reference list. Please check if okay.
- Q4. Please check if supplied definition for “EOV” is appropriate.
- Q5. Please verify if the change to “the long-term effect of the operation” has preserved your meaning.
- Q6. Please verify change of “*W*” to “*w*” to match Eq. (1).
- Q7. Reference [“MSZ 14043/3-79 Hungarian Stand...”] was provided in the reference list; however, this was not mentioned or cited in the manuscript. As a rule, all the references given in the list of references should be cited in the body of a text. Please provide the location of where to insert the reference citation in the main body text.
- Q8. Reference [Ozdemir 2011] was provided in the reference list; however, this was not mentioned or cited in the manuscript. As a rule, all the references given in the list of references should be cited in the body of a text. Please provide the location of where to insert the reference citation in the main body text.